Supporting Information

$K–O_2$ Electrochemistry: Achieving Highly Reversible Peroxide Formation

Philip Heinrich Reinsberg, Andreas Koellisch, Pawel Peter Bawol and Helmut Baltruschat*

Institut für Physikalische und Theoretische Chemie, Universität Bonn, Römerstraße 164, D-53117 Bonn, Germany

*Corresponding author: baltruschat@uni-bonn.de

Table of Contents

Visualization of the Peroxide Oxidation in the Six-Electrode Flow-Through Cell

To visualize the oxidation of the peroxide at a potential of around −1.0 V, two subsequent cycles of the ORR in the dual thin-layer six electrode cell are shown in Figure S1 on a time-scale. The dashed red line in Figure S1 c serves as a guide to the eye and designates to baseline of the experiment.

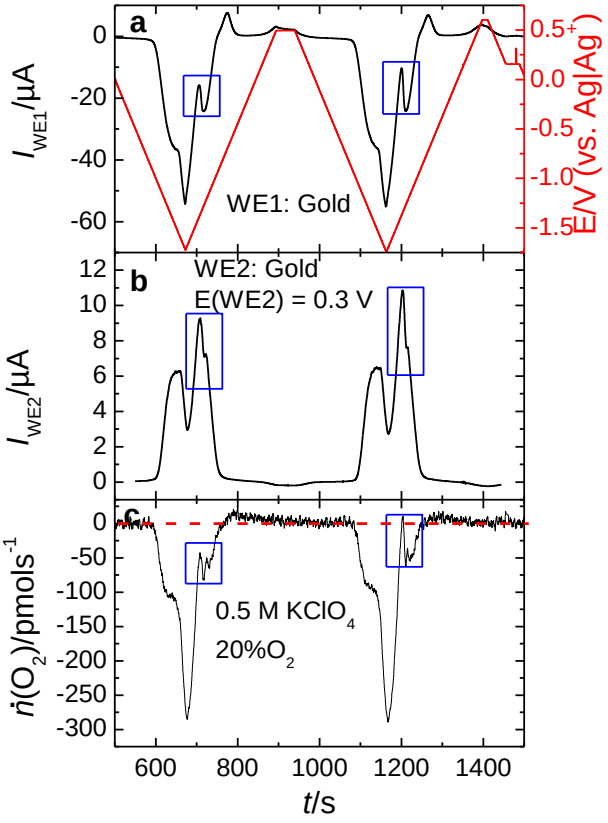

Figure S1: DEMS-measurements employing a 6-electrode dual thin-layer flow cell with two gold working electrodes in a generator-collector arrangement. **a**. Faradaic currents at the generator electrode (WE1) and potentials applied to WE1. **b.** Faradaic currents at the collector electrode (WE2) for a potential of E(WE2) = 0.3 V. **c**. Corresponding flux of oxygen (baseline-corrected). Electrolyte: 0.5 M $KClO_4$ saturated with 20% O_2. Flow rate 5 µL s^{-1}, sweep rate 10 mV s^{-1}. The blue rectangles indicate the oxidation of the peroxide to superoxide and its subsequent oxidation to oxygen at the ring as well as the MS-signal corresponding to this O_2 evolution.

Chronoamperometry in the Flow-Through Cell

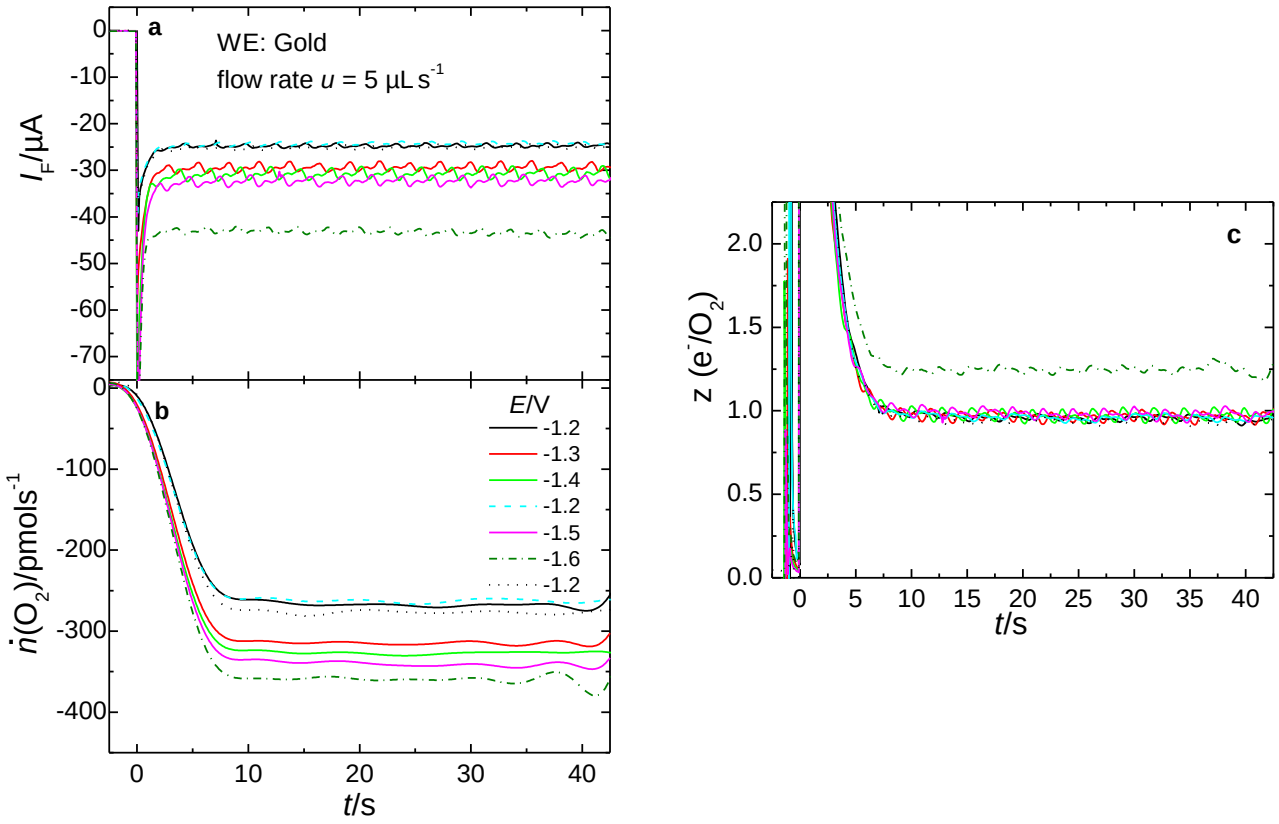

Figure S2: Potential step experiments in a dual thin-layer flow through cell at a gold electrode. **a**. Faradaic currents at the gold electrode. **b**. Corresponding (baseline-corrected) oxygen signal. **c**. Number of electrons transferred per O_2 molecule. Note that the rhythmic noise is due to the peristaltic pump used to maintain electrolyte flow.

From the transients shown Figure S2 no nucleation behaviour is evident, neither for the superoxide nor for the peroxide. Even at a potential of −1.5 V still only one electron is transferred under these experimental conditions.

Determination of the Saturation Concentration of Potassium Superoxide

To determine the saturation concentration of KO_2 in DMSO, two different stock solutions have been prepared. Each solution was produced by adding excess KO_2 to DMSO in an Ar-filled glovebox (*GS Glovebox*) to yield a saturated solution in equilibrium with solid KO_2. Solution *A* was stirred for 1 day at the glovebox temperature (typically 25–27°C) and solution *B* was stirred for 1 day at 40 °C. Each solution was left without stirring for half a day to ensure that the solid particles in the solution precipitate. After that, a fraction of the clear solution was extracted using a syringe with a syringe filter (0.2 µm). To investigate a possible time-effect (due to reaction with trace-amounts of water) on the concentration, solution *B* was stirred for additional 3 days after the extraction and subsequently, an additional fraction was extracted (solution *C*)

The actual determination of the saturation concentration of KO_2 in DMSO was conducted via inductively coupled plasma optical emission spectroscopy (ICP-OES, *PerkinElmer Optima* 8300). Calibration of the instrument was achieved using a multi cation standard (*Merck Certipur* IV, 1000 mg L^{-1}) in four different dilutions (100 µg L^{-1}, 250 µg L^{-1}, 500 µg L^{-1}, 1000 µg L^{-1}) using the K-line at 766 nm (axial detection). The stock solutions *A*–*C* were diluted by a factor of 1000 and 500 to ensure that the measured intensities were within the range of the calibration curve. From the intensities, the saturation concentrations have been calculated (Table S1).

Table S1. Saturation Concentration of K–O_2 in DMSO[a]

	$c(O_2^-)$(1:1000)/mM	Δc/c in %	$c(O_2^-)$(1:500)/mM	Δc/c in %
Solution A	6.34	0.21	6.96	0.16
Solution B	6.87	0.08	6.84	0.18
Solution C	6.89	0.13	6.89	0.14

[a]The saturation concentration has been calculated from the dilution factor. Δc/c represents the relative standard deviation of a series of 6 (1:1000) or 3 (1:500) measurements.

The uncertainty of the values (Δc/c) are given in terms of the relative standard deviation of 6 (1:1000) or 3 (1:500) repeated measurements. As can be seen from Table S1, the saturation concentrations for solutions A–C agree well which each other. No pronounced time- or temperature effect can be observed. From the different measurements a saturation concentration of $c(O_2^-) = 6.77 \pm 0.24 \times 10^{-3}$ mol L^{-1} is calculated and the corresponding solubility constant therefore equals 45.8×10^{-6} mol^2 L^{-2}. Consequently, the saturation concentration of superoxide in a 0.1 M K^+-containing solution equals 0.458 mM (which is well below the saturation concentration of oxygen at atmospheric pressure) or 0.09 mM in a 0.5 M K^+-solution.

Calibration of the Reference Electrode

Due to the presence of diffusion potentials and the fact that the activity coefficient of the silver cations does not equal unity the calculation leading to the values of E^0(vs $Ag^+|Ag$) is not exact.

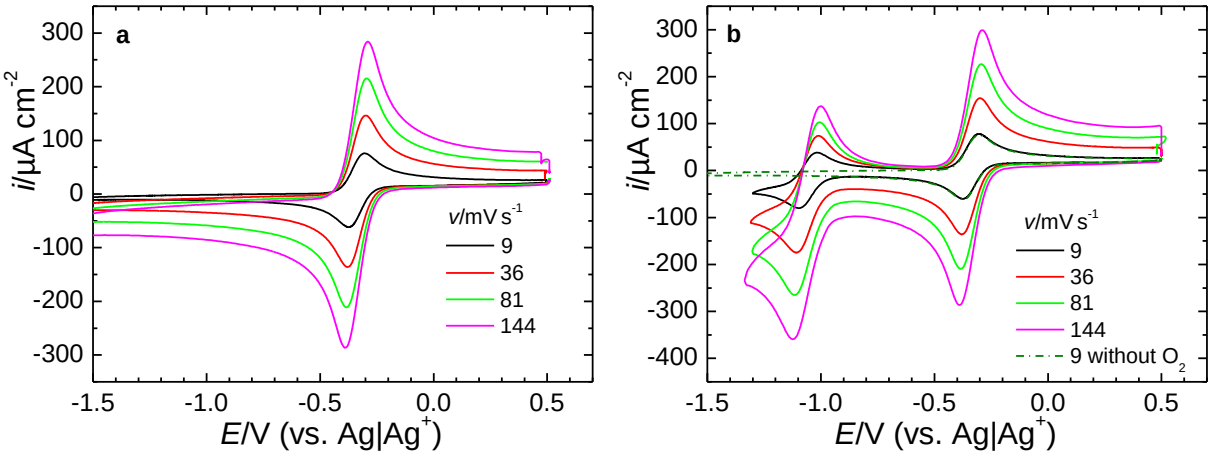

Figure S3: Cyclic voltammetry of the $Me_{10}Fc^+|Me_{10}Fc$ redox couple in 0.1 M $KClO_4$ in DMSO at a glassy carbon electrode. a. In the absence of oxygen. b. In the presence of 20% oxygen. For comparison, the CV in the absence of oxygen at a sweep rate of 9 mV s^{-1} is shown in dark green.

To enhance accuracy as well as comparability to other studies decamethylferrocene was used as a solvent-independent reference. Cyclic voltammograms at a glassy carbon electrode in the absence (Figure S3 a) and presence of O_2 (Figure S3 b) reveal that the $Me_{10}Fc|Me_{10}Fc^+$ expectedly does not depend on the oxygen content. The half-wave potential of the decamethylferrocene couple was determined by averaging the cathodic and anodic peak potential ($E_{1/2} = (E_c+E_a)/2$). The resultant half-wave potential is −0.340 V vs. $Ag^+|Ag$.

Determination of the Diffusion Coefficient of $Me_{10}Fc$ and $Me_{10}Fc^+$

The diffusion coefficient $Me_{10}Fc$ and $Me_{10}Fc^+$ can conveniently be determined performing potential steps at an RRDE: The diffusion coefficient of $Me_{10}Fc^+$ is determined by holding the ring potential at −0.6 V where the reduction of the oxidized species occurs while the disk electrode is suddenly stepped from a potential where no reaction occurs (−0.5 V, 5 s) to a potential where $Me_{10}Fc$ is oxidized (−0.2 V, 11 s). Consequently, the $Me_{10}Fc^+$ produced at the disk will diffuse towards the ring and will lead to reduction current at the ring. From the time delay between disk and ring (t_s), the diffusion coefficient of $Me_{10}Fc^+$ can be evaluated according to eq.(S1) [1], where t_s is in seconds and W^{-1} in rounds per minute:

$$t_s = 43.1\left[\log\left(\frac{r_2}{r_1}\right)\right]^{2/3} \cdot \left(\frac{\nu}{D}\right)^{1/3} \cdot W^{-1} \qquad \text{(S1)}$$

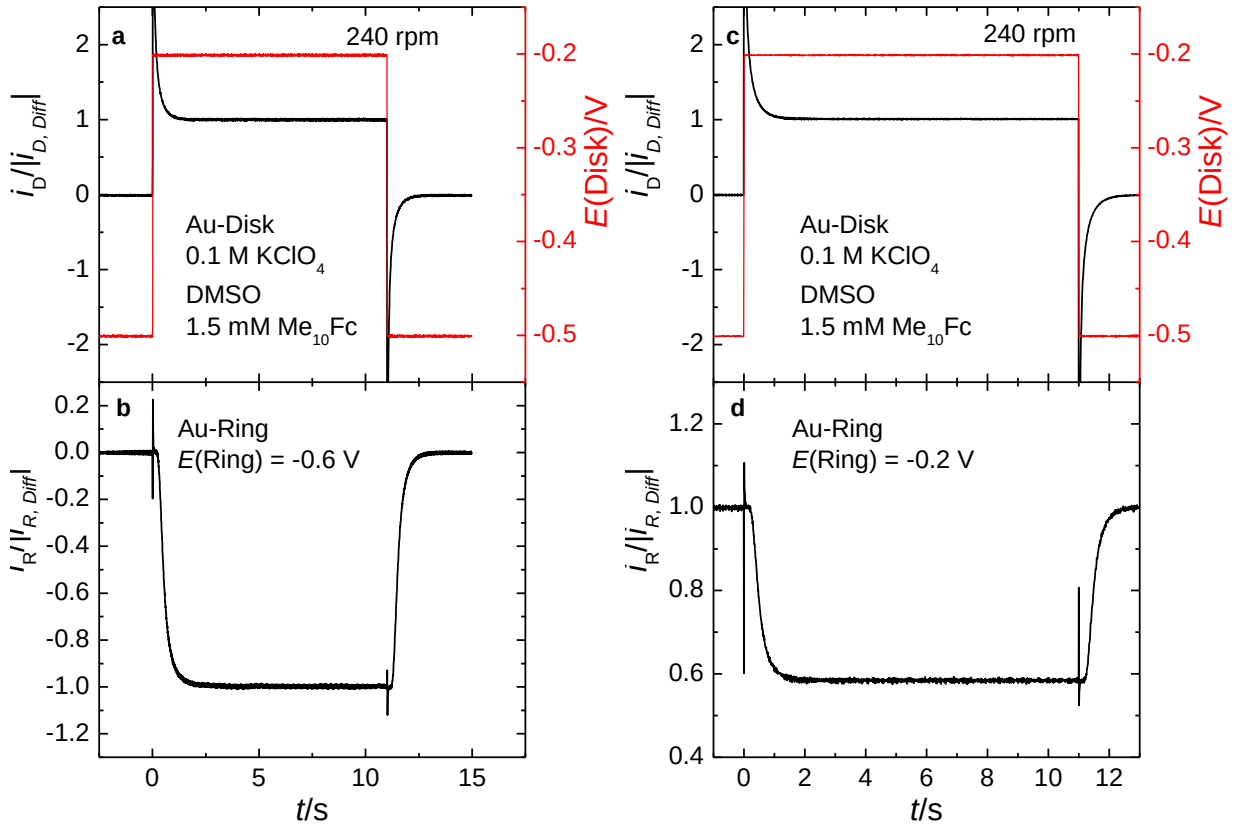

Figure S4: Transients at a thin-gap gold disk- and gold ring-electrode in 0.1 M $KClO_4$ in DMSO containing 1.5 mM $Me_{10}Fc$. a. Disk currents normalized to the constant current in the plateau and the potential applied to the disk (red). b. Ring currents normalized to the constant current in the plateau for a ring potential of −0.6 V, where $Me_{10}Fc^+$ is reduced. c. Disk currents normalized to the constant current in the plateau and the potential applied to the disk (red). d. Normalized ring current for a ring potential of −0.2 V where $Me_{10}Fc$ is oxidized.

In eq. (S1), r_2 is the inner radius of the ring electrode, r_1 is the radius of the disk, ν is the kinematic viscosity, D is the diffusion coefficient of $Me_{10}Fc^+$ and W is the rotation frequency in rounds per minute. The step program as well as the normalized disk and ring currents are shown Figure S5 a and b . The determination of the diffusion coefficient of the neutral species, $Me_{10}Fc$, is carried out via a shielding experiment: A potential of −0.2 V is applied to the ring which leads to an oxidation of $Me_{10}Fc$. The disk potential is stepped from −0.5 V, where no reaction occurs, to −0.2 V and subsequently, $Me_{10}Fc$ is oxidized at the disk electrode. The oxidation of $Me_{10}Fc$ at the disk electrode results in a decrease of the ring current as less $Me_{10}Fc$ is available for oxidation at the ring. From the time delay between disk and ring current, the diffusion coefficient of $Me_{10}Fc$ can be determined according to eq. (S1). The determination of t_s is elucidated in Figure S5 a and b. The dashed line represents a tangent of the turning point of the ring transient and the intercept of the time-axis with the tangent gives the value for t_s at a specific rotation rate. A plot according to eq. (S1) is shown in Figure S5 c.

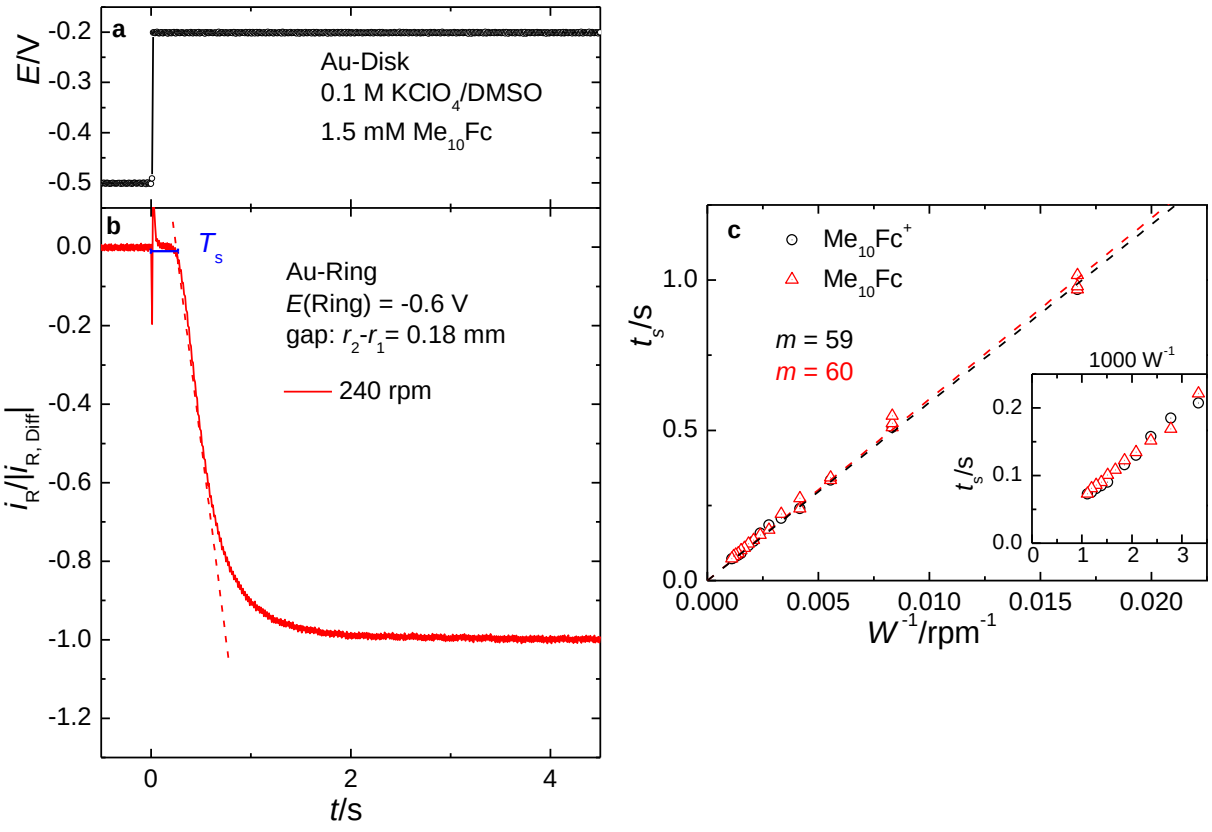

Figure S5: Determination of the transient time t_s. a. Magnification of the potential programme. b. Normalized ring transients for a rotation rate of 240rpm. c. Determination of the diffusion coefficient according to eq. (S1) for $Me_{10}Fc^+$ (black) and $Me_{10}Fc$ (red).

The deviation between the two slopes is well within the experimental error signifying that the diffusion coefficient of both species is identical as expected for a solvent-independent redox system.

Comparison of the Set Ups

The DEMS set up is schematically shown in Figure S6. The electrolyte enters the cell at the upper compartment, where the working electrode 1 (WE1) is placed. The electrolyte then leaves the upper compartment through six, centro-symmetrically aligned capillaries and enters the lower compartment, where a connection to the vacuum of the mass spectrometer (MS) is established via a porous, gold-sputtered Teflon membrane, which serves as the second working electrode (WE2). The electrolyte leaves the cell via a channel connected to the lower compartment. Due to the high electrolyte resistance a set of two reference electrodes (RE) as well as counter electrodes (CE) is necessary. For details refer to Bondue et al. [2]. The time delay between the faradaic current measured at WE1 and the faradaic current at WE2 as well as the signal of the MS is influenced by the thickness of the thin-layer, the length of the capillaries and the flow rate (other factors also play a role but cannot be changed for a given system). Due to the generally high resistances associated with the thin-layer geometry, highly concentrated electrolytes have to be used.

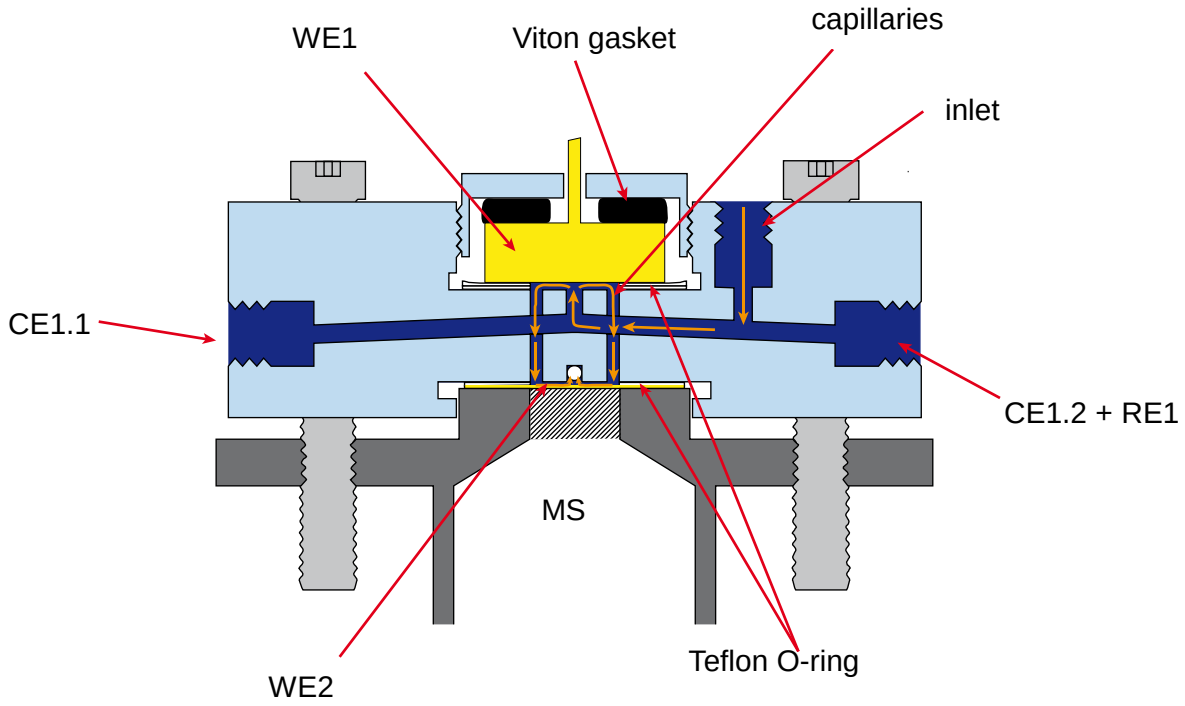

Figure S6: Six electrode dual thin-layer flow through cell.For a detailed description of the cell, refer to the text. Modified after Bondue et al. [2].A diagrammatic sketch an RRDE set up is shown in Figure S7. The RRDE consist of a disk electrode, which is separated via an insulating O-ring from the ring electrode. Both electrodes are mounted into a chemically inert shroud. During an experiment, the whole assembly including the shroud rotates at a rotational frequency ω. The rotational movement of the disk drags the fluid toward its surface. In radial direction, the fluid is pushed from the centre of the disk to the ring electrode. The RRDE set up can also be used for recording simple CVs if the rotation rate is stopped.

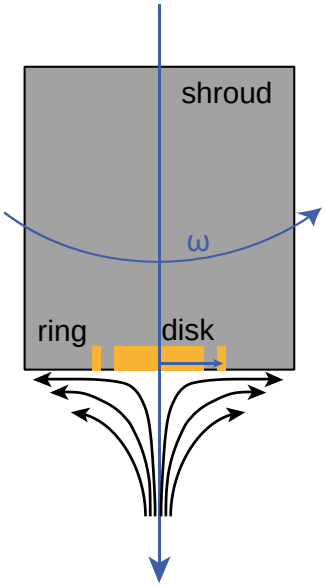

Figure S7: Schematic drawing of the rotating ring-disk electrode. The disk and ring electrode are mounted into non-conducting, chemically inert polytetrafluoroethylene. For a better understanding of the implications of the different set ups, important parameters are given in Table S2. The hypothetical concentration of superoxide close to the surface, $c_{x=0}(O_2^-)$, has been calculated according to eq.(S2) , which is the same as eq. (6) in the main paper.

$$c_{x=0}(O_2^-) = c^0(O_2) \cdot \left(\frac{D(O_2)}{D(O_2^-)} \right)^y \quad \text{(S2)}$$

The coefficient *y* reflects the hydrodynamic conditions and is ½ for the CV measurements[3], and 2/3 in the case of RRDE[3] and DEMS[4] due to the laminar flow conditions. For a derivation of the equation see below.

Table S2: Comparison of different parameters for the different set ups[a]

	$c(KClO_4)$/M	τ/s	$c_{sat}(O_2^-)$	$c_{x=0}(O_2^-)$	$c_{x=0}(O_2^-)/c_{sat}(O_2^-)_t$
DEMS	0.5	2.5	0.09	2.0	22
RRDE	0.1	0.4 (9 Hz)	0.46	2.0	4.5
CV	0.1	NA	0.46	1.4	3.0

[a] $c(KClO_4)$; concentration of $KClO_4$ in the bulk, τ: transfer time between the two working electrodes, $c_{sat}(O_2^-)$: saturation concentration of superoxide calculated from the solubility product of KO_2 ($K_L = 45.8 \times 10^{-6}$ mol²L⁻²), $c_{x=0}(O_2^-)$: concentration at the electrode surface calculated according to eq. (S2) for an oxygen partial pressure of 0.2 bar.

Derivation of Equation 6/Equation S2

Equation 6 or rather eq. (S2) can be derived from the law of mass conservation. In order to conserve mass, the flux of the reactant (R) towards the electrode has to equal the negative flux of the product (P) [3]:

$$J_P(0,t) = -J_R(0,t) \quad \text{(S3)}$$

Using Fick's 1. law of diffusion eq. (S3) can be rewritten using the diffusion coefficients and concentration gradients at the electrode surface:

$$D_P \left[\frac{\partial C_P(x,t)}{\partial x} \right]_{x=0} + D_R \left[\frac{\partial C_R(x,t)}{\partial x} \right]_{x=0} = 0 \quad \text{(S4)}$$

Usually, the concentration gradient in front of the electrode is linearly approximated, which leads to the following expression, where δ_P denotes the thickness of the diffusion layer of the product:

$$D_P \frac{c_{x=0}(P) - c_0(P)}{\delta_P} + D_R \frac{c_{x=0}(R) - c_0(R)}{\delta_R} = 0 \quad \text{(S5)}$$

In the case of diffusion limitation and the initial absence of the product, eq. (S5) simplifies to eq. (S6):

$$D_P \frac{c_{x=0}(P)}{\delta_P} + D_R \frac{-c_0(R)}{\delta_R} = 0 \quad \text{(S6)}$$

Now, only an expression for the thickness of the diffusion-layer is needed. In the case of the RRDE, the diffusion-layer thickness is given by:

$$\delta_P = 1.61 D_P^{1/3} \omega^{-1/2} \nu^{1/6} \quad \text{(S7)}$$

In eq. (S7), ω is the angular frequency and *v* is the kinematic viscosity. Substituting eq. (S7) into eq. (S6) yields:

$$D_P \frac{c_{x=0}(P)}{1.61 D_P^{1/3} \omega^{-1/2} \nu^{1/6}} + D_R \frac{-c_0(R)}{1.61 D_R^{1/3} \omega^{-1/2} \nu^{1/6}} = 0$$

$$D_P \frac{c_{x=0}(P)}{D_P^{1/3}} = D_R \frac{c_0(R)}{D_R^{1/3}} \tag{S8}$$

$$c_{x=0}(P) = c_0(R) \cdot \left(\frac{D_R}{D_P} \right)^{2/3}$$

Comparing eq. (S8) to eq. (S2), with O_2^- = P and O_2 = R, shows that *y* =2/3.

Using the definition of the diffusion-limited current, $I_{Diff} = zFDc_0/\delta$ and the Cottrell-equation ($I_{Diff} = zFD^{1/2}c_0/\pi^{1/2}\ t^{1/2}$), the thickness of the diffusion-layer for semi-infinite diffusion (which is applicable to normal cyclic voltammetry) is given by:

$$\delta_P = \sqrt{\pi D_P t} \tag{S9}$$

Substitution into eq. (S6) and rearrangement leads so the final expression:

$$c_{x=0}(P) = c_0(R) \cdot \left(\frac{D_R}{D_P} \right)^{1/2} \tag{S10}$$

Thus, the exponent *y* equals ½.

Lastly, the expression for the diffusion-limited current in the DEMS-cell at a flow rate *u* of 5 µL s^{-1} (laminar flow) and a geometric factor *g* is given by[4]:

$$I_{Diff} = zF \cdot g \cdot u^{1/3} \cdot c_0 D^{2/3} \tag{S11}$$

Accordingly, the diffusion-layer thickness can be expressed as:

$$\delta_P = D_P^{1/3} u^{-1/3} g^{-1} \tag{S12}$$

Substituting this equation into eq. (S6) again leads to the same expression obtained for the RRDE:

$$c_{x=0}(P) = c_0(R) \cdot \left(\frac{D_R}{D_P} \right)^{2/3} \tag{S13}$$

The similarity between the results for the RRDE and the DEMS originates from the fact that in both cases laminar flow conditions are fulfilled.

References

1. S. Bruckenstein and G. A. Feldman, *Journal of Electroanalytical Chemistry*, 1965, **9**, 395-399.
2. C. J. Bondue, P. Königshoven and H. Baltruschat, *Electrochim. Acta*, 2016, **214**, 241–252.
3. A. J. Bard and L. R. Faulkner, *Electrochemical Methods: Fundamentals and Applications*, John Wiley & Sons Inc., New York, Weinheim, 2nd edn., 2001.
4. M. Khodayari, P. Reinsberg, A.-E.-A. A. Abd-El-Latif, C. Merdon, J. Fuhrmann and H. Baltruschat, *ChemPhysChem*, 2016, **17**, 1647-1655.